

Research

Microwave-assisted selective oxidation of propene over bismuth molybdate catalysts: the importance of catalyst synthesis methodology

Jia Sun¹ · James S. Hayward¹ · Michael Barter² · Daniel R. Slocombe² · Jonathan K. Bartley¹

Received: 31 October 2024 / Accepted: 26 May 2025

Published online: 23 June 2025

© The Author(s) 2025 [OPEN](#)

Abstract

A series of bismuth molybdate catalysts were synthesised at different pH via a hydrothermal method using citric acid. The calcined and uncalcined catalysts were tested for the selective oxidation of propene to acrolein under microwave-electric field heating and conventional heating. Under conventional heating the catalysts synthesised at low pH were found to give the best performance, however, under microwave heating the key parameter was the calcination step. The dielectric properties were determined using cavity perturbation methods and non-calcined samples were found to have a high dielectric loss tangent, a measure of how well a material can convert microwave radiation into heat, that was ascribed to residual water and nitrate ions in the catalysts. On calcination the residual water and nitrate was removed and the particle size increased leading to low dielectric loss tangents. When heated at low power (10–20 W) the microwave-electric field the catalysts gave very high selectivity to acrolein compared to the conventionally heated catalysts at isoconversion. This was attributed to the microwave energy selectively heating the catalyst bed, but not the reactants, suppressing sequential oxidation and cracking reactions. This study demonstrates the importance of both the materials dielectric and catalytic properties in microwave-assisted catalysis which allows high yields to be achieved when compared to the same catalysts under conventional heating.

1 Introduction

Microwave-assisted catalysis is becoming increasingly studied for both liquid and gas phase chemical reactions. Previous studies have shown that there are several potential advantages of microwave heating compared to conventional heating, including the creation of hot spots and microwave plasmas on the catalyst surface and the selective heating of catalysts, reactants, or solvents which can give higher reaction rates and improve the activity and/or selectivity of processes [1–4].

Some of these advantages could be useful if microwave-assisted catalysis was applied to selective oxidation reactions. For example, gas phase reactants cannot be heated in the microwave field and the microwave energy is only used to heat the catalyst bed. This can be beneficial in improving energy efficiency and reducing sequential gas phase reactions, increasing the selectivity of the process studied [5]. However, the formation of hot spots on the catalysts can be a disadvantage as these promote high temperatures and over oxidation of the products.

Supplementary Information The online version contains supplementary material available at <https://doi.org/10.1007/s44344-025-00014-7>.

✉ Jonathan K. Bartley, BartleyJK@cardiff.ac.uk | ¹Cardiff Catalysis Institute, School of Chemistry, Cardiff University, Cardiff, UK. ²Centre for High Frequency Engineering, School of Engineering, Cardiff University, Cardiff, UK.



In this study we have explored the role of the catalysts in microwave-assisted catalysis using propene oxidation as a model reaction. There are several possible reaction products including acrolein, acetaldehyde, formaldehyde, carboxylic acids and carbon oxides, which makes it an interesting candidate for comparing activity and selectivity between microwave and conventional heating.

In this study bismuth molybdate was chosen as the catalyst, with three phases ($\text{Bi}_2\text{Mo}_3\text{O}_{12}$, $\text{Bi}_2\text{Mo}_2\text{O}_9$, and Bi_2MoO_6) known to have good performance for the oxidation/ammoxidation of lower alkenes [6]. This allows the different phases to be studied as both catalysts and microwave susceptors to gain information on the importance of these two properties of the materials. Early studies on propene selective oxidation found that both pure phase MoO_3 and Bi_2O_3 showed promising activity, but when combined as bismuth molybdate a considerable improvement in performance was observed [7, 8]. Many investigations identifying the order of relative activity of bismuth molybdate phases have been published over the past few decades. However, there is still debate in the literature about the relative activity of these bismuth molybdate phases. Early studies reported that $\text{Bi}_2\text{Mo}_2\text{O}_9$ was more active for propene oxidation than the other two bismuth molybdate phases [9–11], while other researchers suggested that Bi_2MoO_6 [12] or $\text{Bi}_2\text{Mo}_3\text{O}_{12}$ were more active catalysts [13]. It is generally agreed that bismuth-based catalysts containing vanadium, molybdenum, bismuth, magnesium and antimony are among the most active catalysts providing redox sites for the reaction, and that the reaction proceeds through a Mars van Krevelen type mechanism, where lattice oxygen plays the key role in the catalytic activity for propene selective oxidation [14].

In a previous study, we investigated a series of bismuth molybdate vanadate materials with different ratios of molybdenum to vanadium that were synthesised using a sol–gel methodology using citric acid [15]. Here we build on these initial results by investigating hydrothermal synthesis as a methodology for producing active microwave-assisted bismuth molybdate catalysts.

2 Experimental section

2.1 Catalyst synthesis

A group of bismuth molybdate materials were prepared using hydrothermal synthesis at different pH. 2.425 g of $\text{Bi}(\text{NO}_3)_3 \cdot 5\text{H}_2\text{O}$, and 0.606 g of $\text{Na}_2\text{MoO}_4 \cdot 2\text{H}_2\text{O}$ were dissolved into 5 ml of HNO_3 (4 M). A concentrated aqueous solution of NaOH (2 M) was added dropwise into the solution until the target pH value was reached. After being stirred for 2 h, the suspension was transferred into a 100 mL Teflon-lined stainless-steel autoclave to 70% of the total volume. The autoclave was heated at 160 °C for 24 h at autogenous pressure and then allowed to cool to room temperature. The resulting samples were separated by filtration, washed with 100 ml deionized water and 100 ml absolute alcohol several times, and then dried at 110 °C overnight. The samples synthesised at pH 4, 6 and 8 were denoted BiMoOx-4, BiMoOx-6 and BiMoOx-8 respectively.

The materials were tested as synthesised and also after calcination in static air at 500 °C with a ramp rate of 5 °C min^{-1} . The calcined materials were denoted BiMoOx-4C, BiMoOx-6C and BiMoOx-8C.

3 Catalyst characterisation

3.1 X-ray diffraction (XRD)

Analysis was carried out using a PANalytical X'pert Pro powder diffractometer with a $\text{Cu K}_{\alpha 1}$ X-ray radiation ($\lambda = 0.154098$ nm) source at ambient temperature. Samples were typically scanned in the range of 10–80° at 40 kV and 40 mA. Samples were ground and placed into a backfilled sample holder for analysis. Crystal structures were assigned using MDI/Jade software using the International Centre for Diffraction Data (ICDD) database from the Powder Diffraction File (PDF).

3.2 Surface area analysis

Nitrogen adsorption isotherms were collected using a Quantachrome Quadrasorb evo surface area analyser at $-196\text{ }^{\circ}\text{C}$. A five point plot was performed using N_2 as the adsorbate gas. Samples were degassed under vacuum at $150\text{ }^{\circ}\text{C}$ for 3 h before analysis. Surface areas were calculated using the BET method over the p/p_0 range of 0.05–0.3, using QuadraWin software.

3.3 X-ray photoelectric spectroscopy (XPS)

XPS analysis was carried out using a Kratos Axis Ultra-DLD spectrometer, utilizing a micro-focused monochromatic Al K_α X-ray source ($h\nu = 1486.6\text{ eV}$) operating at 72 W power. Samples were analysed at pass energies of 40 and 150 eV for high-resolution and survey scans, respectively. A C1s reference (284.5 eV) was used to correct the charge effect. Data analysis was performed in CasaXPS software using a Shirley-type background and Scofield cross-sections.

3.4 Inductively coupled plasma mass spectrometry (ICP-MS)

Analysis was carried out using an Agilent 7900 ICP-MS instrument, equipped with a micro-mist nebuliser in organic phase mode. Quantification was carried out by comparison with a calibration curve.

3.5 Characterisation of dielectric properties

The cavity perturbation method was used to measure the dielectric parameters using methodology described previously [15–19]. Dielectric properties analyses were carried out using a cyl- ϵ cavity [18]. TM_{010} modes were used to measure the dielectric properties of a tube sample placed on the axis. The resonance frequency and Q-factor of the cavity were measured with an empty tube, and with samples inserted. The real part and imaginary part of the complex permittivity were calculated and used to determine the loss tangent ($\tan \delta$) that is used to provide an indication of how the material can be penetrated by an electric field and how it dissipates the energy as heat.

3.6 Thermal gravimetric analysis (TGA)

Analysis was carried out using a Seteram TGA/DTA. Samples were placed in a pre weighed crucible and heated from 30 to $800\text{ }^{\circ}\text{C}$ under an air flow (30 ml min^{-1}) at a heating rate of $1\text{ }^{\circ}\text{C min}^{-1}$.

3.7 Product analysis

Products were collected and analyzed using an online gas chromatograph (Agilent 7680A) equipped with an HP-PlotQ ($30\text{ m} \times 0.530\text{ mm}$) column and a Porapak Q (80–100 Mesh, $1.8\text{ m} \times 2.0\text{ mm}$) column for separation of the products, and flame ionization detector (FID) and thermal conductivity detector (TCD) for analyzing the products.

3.8 Evaluation of catalytic performance

The catalytic performance of the prepared catalysts was evaluated for the selective oxidation of propene to acrolein at atmospheric pressure in a laboratory fixed bed reactor using either conventional or microwave dielectric heating using methodology described previously [15].

0.2 g of catalyst was placed in a quartz reactor tube (7 mm internal diameter) held between plugs of quartz wool. Propene, nitrogen and oxygen were introduced using mass flow controllers (Bronkhorst) to give a total flow rate of 50 ml min^{-1} (propene: O_2 :He = 5:10:85). The outlet lines were heated to $140\text{ }^{\circ}\text{C}$ to prevent condensation of the products. Products were analysed using online gas chromatography.

For conventional heating experiments ($200\text{--}500\text{ }^{\circ}\text{C}$) the reactor was placed in a tube furnace (LPC Elements) and the temperature was monitored using a thermocouple at the centre of the catalyst bed.

For experiments carried out using microwave dielectric heating a TM_{010} single-mode microwave cavity. A quartz reactor tube was located in the middle of the cavity. The catalyst bed was irradiated with 2.5 GHz microwave radiation with a power of 0–30 W through a hole in the side of the cavity perpendicular to the catalyst bed. On the opposite side of the

Fig. 1 XRD patterns of bismuth molybdate materials hydrothermally synthesized at different pH and after calcination at 500 °C, together with the reference patterns for Bi_2MoO_6 (PDF#072-1524) and Bi_4MoO_9 (PDF#012-0149)

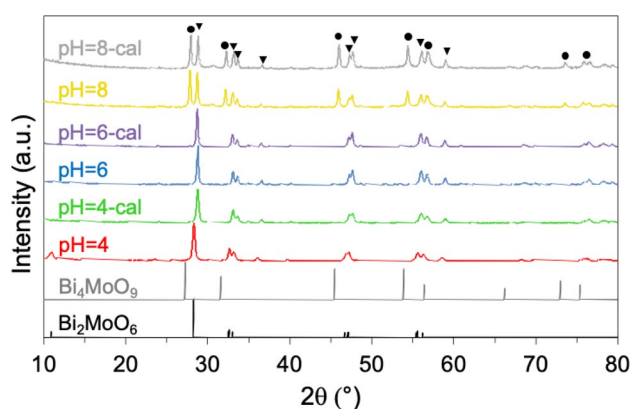


Table 1 Crystallite size and lattice constants for samples synthesised at different pH calculated from the (131) reflection of Bi_2MoO_6 from the XRD patterns in Fig. 1

| Material | Crystallite Size (nm) ^a | Lattice Parameters | | | | |
|-----------|------------------------------------|--|--------------|--------------|--------------|--------------------------|
| | | | <i>a</i> (Å) | <i>b</i> (Å) | <i>c</i> (Å) | Volume (Å ³) |
| BiMoOx-4 | 22.6 | Orthorhombic Bi_2MoO_6 | 5.54 | 16.23 | 5.50 | 494 |
| BiMoOx-6 | 33.7 | Orthorhombic Bi_2MoO_6 | 5.50 | 16.34 | 5.47 | 492 |
| BiMoOx-8 | 45.6 | Orthorhombic Bi_2MoO_6 | 5.49 | 16.20 | 5.48 | 488 |
| | | Cubic Bi_4MoO_9 | 5.63 | 5.63 | 5.63 | 179 |
| BiMoOx-4C | 25.1 | Orthorhombic Bi_2MoO_6 | 5.50 | 16.20 | 5.46 | 488 |
| BiMoOx-6C | 36.6 | Orthorhombic Bi_2MoO_6 | 5.50 | 16.29 | 5.47 | 491 |
| BiMoOx-8C | 46.7 | Orthorhombic Bi_2MoO_6 | 5.48 | 16.20 | 5.46 | 487 |
| | | Cubic Bi_4MoO_9 | 5.63 | 5.63 | 5.63 | 179 |

^acrystallite size calculated using the (131) reflection of Bi_2MoO_6

cavity, an infrared camera was mounted to detect the temperature of the catalyst bed when steady state was achieved (Figure S1) [15].

Products were collected and analyzed using an online gas chromatograph (Agilent 7680A) equipped with an HP-PlotQ (30 m × 0.530 mm) column and a Porapak Q (80–100 Mesh, 1.8 m × 2.0 mm) column for separation of the products, and flame ionization detector (FID) and thermal conductivity detector (TCD) for analyzing the products. Conversion and selectivity were calculated using the equations below:

$$\text{Propene conversion (\%)} = (\text{moles of propene in} - \text{moles of propene out}) / \text{moles of propene in} \times 100\%.$$

$$\text{Product selectivity (\%)} = \text{moles of specific product} / \text{moles of total products} \times 100\%.$$

4 Results and discussion

4.1 Catalyst characterisation

The bismuth molybdate materials synthesised at different pH (4, 6 and 8) and their calcined counterparts were characterised using a combination of techniques.

The XRD patterns revealed that a low pH solution resulted in the formation of orthorhombic Bi_2MoO_6 , while higher pH gave a mixed phase of orthorhombic Bi_2MoO_6 and cubic Bi_4MoO_9 structures. This observation is similar to the findings of Phurangrat et al. [20] who synthesized a set of Bi_2MoO_6 materials using hydrothermal synthesis and investigated the effect of the precursor solution pH on the phases formed, morphologies, and photocatalytic activity. They found that low pH (< 7) contributed to the formation of orthorhombic Bi_2MoO_6 , medium pH (8–10) gave a mixed phase of orthorhombic Bi_2MoO_6 and cubic Bi_4MoO_9 structures and high pH (> 10) led to the formation of cubic Bi_4MoO_9 .

The average crystallite size was calculated using the Debye–Scherrer equation considering the broadening of the (131) reflection of Bi_2MoO_6 in the XRD patterns (Fig. 1) and the results are shown in Table 1. The materials showed an increase in the crystallite size with an increase in the pH of the reaction mixture. Similar results were also found by Bakiro et al. when

Table 2 Surface area and composition of the bismuth molybdate materials hydrothermally synthesized at different pH

| Material | Surface area (m ² g ⁻¹) | Bi/Mo bulk ratio ^a | Bi/Mo surface ratio ^b |
|-----------|--|-------------------------------|----------------------------------|
| BiMoOx-4 | 16 | 2.1 | 2.1 |
| BiMoOx-6 | 17 | 2.2 | 2.4 |
| BiMoOx-8 | 25 | 3.2 | 3.8 |
| BiMoOx-4C | 14 | 2.1 | 2.4 |
| BiMoOx-6C | 14 | 2.2 | 2.5 |
| BiMoOx-8C | 19 | 3.3 | 4.0 |

^adetermined from ICP-MS^bdetermined from XPS**Table 3** Dielectric parameters for bismuth molybdate materials hydrothermally synthesized at different pH

| Material | Dielectric constant (ϵ') | Dielectric loss (ϵ'') | Loss tangent ($\tan \delta$) |
|-----------|-------------------------------------|----------------------------------|--------------------------------|
| BiMoOx-4 | 1.0016 | 0.14135 | 0.14128 |
| BiMoOx-6 | 1.0014 | 0.12841 | 0.12823 |
| BiMoOx-8 | 1.0016 | 0.12691 | 0.12671 |
| BiMoOx-4C | 1.0012 | 0.05607 | 0.05600 |
| BiMoOx-6C | 1.0013 | 0.04210 | 0.04205 |
| BiMoOx-8C | 1.0013 | 0.04194 | 0.04189 |

synthesising BiNbO₄ [21]. They reported that high pH is attributed to the increase crystallite size due to agglomeration resulting in the preferential formation of β -BiNbO₄ at the expense of α -BiNbO₄ at high pH. In Phuruangrat's studies of Bi₂MoO₆ synthesis, a similar conclusion was also reported, with acidic conditions favouring the formation of Bi₂MoO₆, and alkaline conditions leading to larger crystallite sizes of Bi₂MoO₆ and the formation of Bi₄MoO₉ [20].

BET surface areas were determined by N₂ adsorption and were found to correlate with the particle sizes determined by XRD, with calcination leading to a reduction in surface area and an increase in particle size, brought about by sintering. The surface bismuth/molybdenum compositions were determined using X-ray photoelectron spectrometry (XPS) and the bulk composition of the catalysts was determined by optical emission spectrometry with inductively coupled plasma (ICP-MS). The specific surface area of the samples and the Bi/Mo ratios determined by ICP-MS and XPS are summarized in Table 2, with XPS spectra provided in the supporting information (Figures S2-S7).

Samples synthesized in higher pH solutions contain a higher amount of Bi, both in the bulk and on the surface. This is in line with the XRD results, that showed that large amounts of Bi rich phase Bi₄MoO₉ were produced by the higher pH precursor solution. A similar result was also reported by Schuh et al. who synthesized a group of bismuth molybdate from solutions with different pH using a hydrothermal method [17]. The calcination did not have a significant effect on the Bi/Mo ratio of the catalyst in the bulk, but the XPS results revealed that the calcination process increased the bismuth content on the catalyst surface. This has been ascribed to a bismuth rich surface layer that has been shown to form on the surface of bismuth molybdate materials after calcination [22], but is not considered crucial to the performance as the catalysts equilibrate under reaction conditions [22, 23].

When considering potential materials for use as microwave-assisted catalysts using electric field heating, the interaction of materials with microwaves and the heating behaviour of materials by microwave irradiation is strongly dependent on their dielectric properties. The complex permittivity of a material is related to the dielectric constant (ϵ'), the ability of a material to hold electric charge, and the dielectric loss factor (ϵ'') which is related to how well a material converts energy into heat. Commonly these properties are summarised by the loss tangent ($\tan \delta = \epsilon''/\epsilon'$) which is used as an indicator of how well a material can be heated in a microwave-electric field. The dielectric properties were measured using a cylindrical cavity operating at 2.5 GHz with TM₀₁₀ mode as described previously [15–19] and are shown in Table 3.

The dielectric properties obtained indicate that the non-calcined samples are more likely to reach higher temperatures than the calcined samples due to the differences in dielectric loss. This is ascribed to the presence of water of crystallinity or other impurities like NO₃⁻ in the sample structure that can facilitate microwave absorption at the very beginning of microwave heating, as the water and NO₃⁻ usually have larger polarity than bismuth molybdate and are usually

Fig. 2 TGA for non-calcined and calcined bismuth molybdate materials hydrothermally synthesised at pH 4

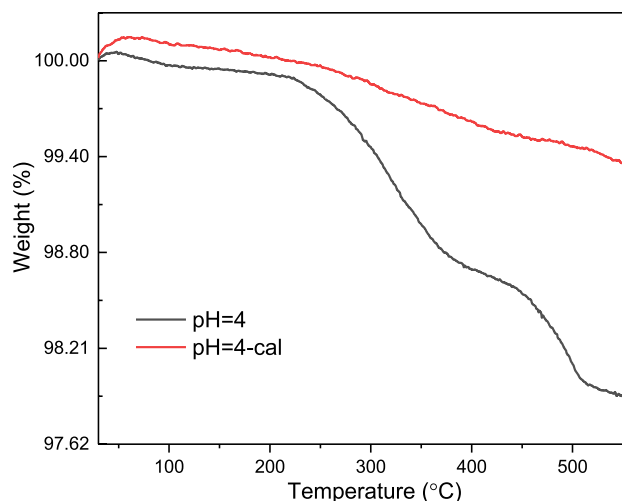
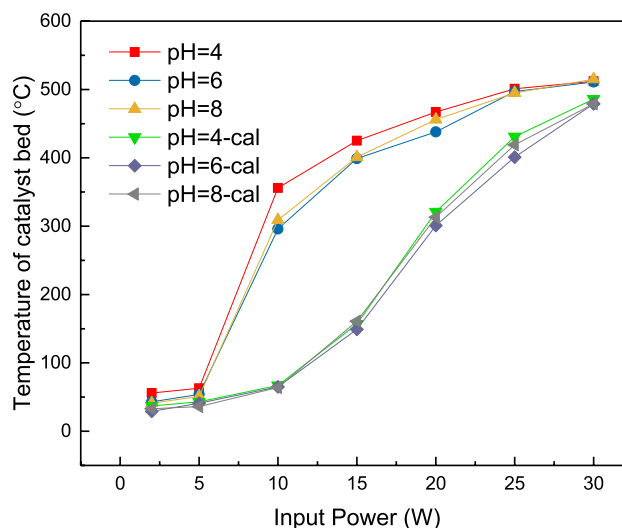


Fig. 3 Temperature of the catalyst bed under microwave heating in air



better at utilizing the microwave energy and become dielectric loss. Due to the excellent dielectric properties, bismuth nitrate salts have been used in microwave synthesis of naphthyridines [24], microwave-assisted synthesis of molecules of medicinal interest [25], and to catalyse a unique route to produce 1,4-dihydropyridines [26].

Thermal gravimetric analysis was carried out on the BiMoOx-4 and BiMoOx-4C materials to identify any impurities present in the as synthesised material compared to the calcined material (Fig. 2). The non-calcined sample shows a much larger weight drop than the calcined sample with two clear weight-loss stages. The first loss at 250–300 °C corresponds to the removal of water [27], while the second weight loss from 400 to 500 °C is in the region expected from the decomposition of bismuth nitrate salts [28].

However, as evidenced by the XRD and surface area measurements, calcination also leads to an increase in crystallinity and particle size and a decrease in the surface area. The mechanism of microwave heating for solids is dependent on the domain sizes as they align with the oscillating electric field, so the increase in domain size on calcination will also impact on how well the materials can be heated.

4.2 Catalyst testing

The catalytic activity of the bismuth molybdate samples for the selective oxidation of propene was tested under both conventional and microwave heating. Initially, catalysts were heated in the microwave cavity with power ranging from 2.5 W to 30 W and the temperature of the catalyst bed was measured remotely using an infrared (IR) camera (Fig. 3). The IR camera measurement is not as accurate as the thermocouple inserted into the bed during conventional heating, as it

does not account for localised hot spots and can underestimate bed temperature. However, inserting a thermocouple will impact on the microwave heating regime within the catalyst bed. All samples could be heated in the microwave field to greater than 450 °C and so were good candidates as catalysts for the microwave-assisted oxidation of propene. However, the non-calcined samples reached higher temperatures at lower microwave power due to their much higher dielectric loss tangents which indicate their ability to convert microwave energy into heat (Table 3).

Although both the water and nitrate ions in the samples will be removed when the temperature reaches a high level (300 °C and 450 °C, respectively), their positive effect on improving the temperature in the initial heating stage is still very important to assist the bulk catalyst to reach a higher temperature. In the initial heating stage, water and NO_3^- can absorb a large amount of microwave energy and transfer heat to the surrounding catalyst which result in a pre-heating effect on the catalyst bed. An investigation studying the dielectric properties of heterogeneous catalysts have shown that the dielectric loss is highly temperature dependent [29]. When catalysts were preheated using conventional heating the loss tangent was found to increase with increasing temperature [29, 30]. At a higher temperature, the mobility of charge carriers in the solid solution materials will be higher, which increases the polarization of the materials that leads to high dielectric loss [21]. Therefore, pre-heating the catalyst in advance is beneficial for the catalyst to absorb more microwave energy.

The performance of the prepared catalysts were also evaluated under conventional heating in a flow of propene, oxygen, and nitrogen from 200 °C to 500 °C. The results are shown in Figs. 4 and 5, with the full product selectivity shown in Table 4.

Under conventional heating the non-calcined samples showed higher activity and selectivity than the corresponding calcined samples. The reduction in performance is attributed to the increase in crystallite size and decrease of the surface area of the materials when calcined, leading to less active sites available in the calcined catalysts. According to the ICP and XPS results (Table 2) materials synthesized at higher pH contains a larger amount of bismuth, both in the bulk and on the surface, and the calcination process increased the bismuth content on the catalyst surface. In the mechanism for propene selective oxidation [10], the adsorption of propene is proposed to occur on a molybdenum site, that is reduced during acrolein formation, implying the surface Mo concentration is crucial for bismuth molybdate to maintain high selectivity to acrolein. The increase in surface bismuth sites makes the catalyst more inclined to produce carbon dioxide at higher temperature, which has been reported by previous researchers for propene selective oxidation over the bismuth molybdate catalysts [31–33].

The catalyst synthesised at pH 4 (BiMoOx-4) performed best under conventional heating with a maximum acrolein selectivity of 82% reached at 300 °C. The corresponding calcined sample (BiMoOx-4c) showed the next best performance, indicating that under conventional heating the pH, that controls the phase composition, is the most important synthesis parameter. For the materials synthesised at pH 6 and pH 8, both the conversion and selectivity to acrolein were found to be much lower than the catalysts synthesised at pH 4. For the catalyst synthesised at pH 6 acetaldehyde was the major product detected, while the catalysts synthesised at pH 8 gave acetaldehyde at low temperatures, but non-oxygenated products were the major product at high conversion. The by-products of the reaction were CO_2 and CO, with very small

Fig. 4 Propene conversion under conventional heating (0.2 g of catalyst, propene:oxygen:nitrogen = 1:2:97, flow rate = 50 mL min⁻¹)

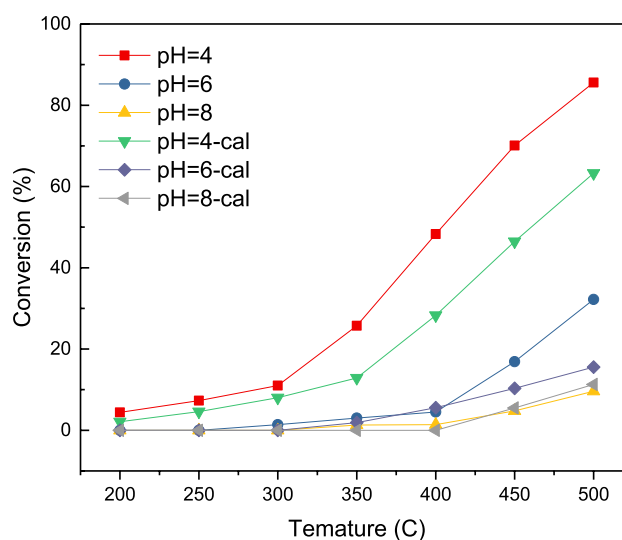
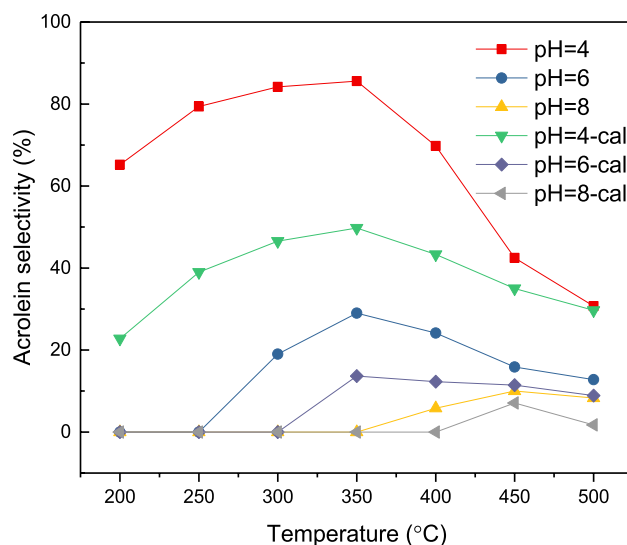


Fig. 5 Acrolein selectivity under conventional heating (0.2 g of catalyst, propene:oxygen:nitrogen = 1:2:97, flow rate = 50 mL min⁻¹)



amounts of other C₃ oxygenates, and ethene and hexadiene observed at temperatures above 500 °C (Table 4). The poorer performance is attributed to the increase in the formation of the bismuth rich phase (Bi₄MoO₉) as the pH increases as observed by XRD. This agrees with the early research by Martir and Lunsford that found that over Bi₂O₃ catalysts, the major reaction product is 1,5-hexadiene, as there is less lattice oxygen available in bismuth oxide than in bismuth molybdate, which is crucial for the Mars van Krevelen reaction mechanism [34]. Schuh et al. also reported similar findings for a series of bismuth molybdate catalysts prepared at different pH and Bi:Mo ratios with low propene conversion and acrolein selectivity over bismuth rich catalysts [35].

The bismuth molybdate catalysts were then tested under the same reaction conditions but using microwave-dielectric heating and the results shown in Figs. 6 and 7 and Table 5.

As shown in Fig. 6, all of the hydrothermally synthesized Bi₂MoO₆ samples showed activity under microwave heating. The trend in the propene conversion at different microwave power is similar to the catalyst bed temperature reached at different microwave powers shown in Fig. 3. As the uncalcined samples can reach higher temperatures at lower microwave power, the three uncalcined catalysts give higher conversion than the corresponding calcined catalysts, especially at low power. However, there is a clear performance advantage for the catalyst synthesised at pH 4 (BiMoOx-4) over those calcined at pH6 and 8 (BiMoOx-6 and BiMoOx-8) indicating that the conversion is not just related to the permittivity of the materials, but is also dependent on traditional catalyst properties such as the nature of the active sites. Comparing the activity under microwave heating (Fig. 6) with the activity under conventional heating (Fig. 4) and the bed temperature at different microwave power (Fig. 3) shows that the behaviour is clearly a combination of the catalytic and dielectric properties.

The selectivity to acrolein under microwave heating is shown in Fig. 7. The selectivity to acrolein reaches a maximum at 10 W microwave power for all the catalysts, before dropping linearly with power until there is no acrolein produced at 30 W. Although this drop is more pronounced than in conventional heating, the conversion at maximum selectivity under microwave heating is much higher for all the catalysts tested. This confirms that for selective oxidation, the proposed advantages over conventional heating of increased selectivity due to limiting secondary reactions, coupled with the higher conversions achieved under microwave heating of the catalyst bed gives improved performance.

This is confirmed by a comparison of the acrolein yields under the different heating regimes (Figs. 8 and 9), where the maximum yield is higher for all catalysts under microwave heating. To demonstrate this is not simply a heating effect a comparison of the best catalyst (BiMoOx-4) under microwave and conventional heating is given in Fig. 10. Under conventional heating the catalyst showed typical behaviour with a drop in selectivity as conversion increases (Figs. 4 and 5) leading to a maximum yield of around 25%. However, under microwave heating the higher selectivity achieved at high conversion give much higher yields (> 50%) than can be achieved under conventional heating.

Product selectivity is critical in catalytic processes as it allows for simpler separation of products, and minimises downstream waste. To accurately compare the selectivity of different catalysts it is crucial to compare them at isoconversion [36, 37]. The selectivity is dependent on the conversion and for consecutive reactions can be the relative selectivity is dependent on the rate of the individual steps. This is particularly true of batch reactions, where an intermediate can

Table 4 Selectivity of the main products from propene oxidation under conventional testing

| Sample | Temperature (°C) | Selectivity (%) | | | | |
|-----------|------------------|-----------------|--------------|-----------------|----------------------------------|---------------------------------|
| | | Acrolein | Acetaldehyde | CO _x | Higher hydrocarbons ^a | Lower hydrocarbons ^b |
| BiMoOx-4 | 200 | 65 | 0 | 0 | 0 | 0 |
| | 250 | 76 | 7 | 0 | 0 | 0 |
| | 300 | 89 | 7 | 0 | 0 | 3 |
| | 350 | 81 | 6 | 0 | 6 | 3 |
| | 400 | 46 | 5 | 9 | 23 | 10 |
| | 450 | 42 | 8 | 11 | 13 | 23 |
| | 500 | 31 | 8 | 13 | 3 | 41 |
| BiMoOx-4C | 200 | 23 | 0 | 0 | 0 | 0 |
| | 250 | 27 | 7 | 0 | 0 | 0 |
| | 300 | 40 | 7 | 0 | 0 | 3 |
| | 350 | 41 | 5 | 0 | 6 | 3 |
| | 400 | 46 | 5 | 9 | 23 | 10 |
| | 450 | 50 | 8 | 10 | 13 | 23 |
| | 500 | 30 | 7 | 13 | 3 | 41 |
| BiMoOx-6 | 200 | 0 | 0 | 0 | 0 | 0 |
| | 250 | 0 | 0 | 0 | 0 | 0 |
| | 300 | 12 | 13 | 0 | 0 | 2 |
| | 350 | 11 | 19 | 0 | 0 | 3 |
| | 400 | 11 | 33 | 0 | 0 | 4 |
| | 450 | 13 | 36 | 5 | 5 | 26 |
| | 500 | 43 | 2 | 9 | 3 | 45 |
| BiMoOx-6C | 200 | 0 | 0 | 0 | 0 | 0 |
| | 250 | 0 | 0 | 0 | 0 | 0 |
| | 300 | 0 | 16 | 0 | 0 | 3 |
| | 350 | 14 | 19 | 0 | 0 | 3 |
| | 400 | 12 | 31 | 0 | 0 | 4 |
| | 450 | 14 | 37 | 4 | 5 | 27 |
| | 500 | 39 | 3 | 8 | 3 | 45 |
| BiMoOx-8 | 200 | 0 | 0 | 0 | 0 | 0 |
| | 250 | 0 | 0 | 0 | 0 | 0 |
| | 300 | 0 | 0 | 0 | 0 | 0 |
| | 350 | 0 | 20 | 0 | 0 | 20 |
| | 400 | 6 | 4 | 0 | 0 | 27 |
| | 450 | 10 | 3 | 10 | 47 | 21 |
| | 500 | 8 | 3 | 5 | 79 | 2 |
| BiMoOx-8C | 200 | 0 | 0 | 0 | 0 | 0 |
| | 250 | 0 | 0 | 0 | 0 | 0 |
| | 300 | 0 | 0 | 0 | 0 | 0 |
| | 350 | 0 | 22 | 0 | 0 | 0 |
| | 400 | 0 | 2 | 0 | 0 | 0 |
| | 450 | 5 | 1 | 11 | 10 | 47 |
| | 500 | 11 | 2 | 17 | 5 | 79 |

^aHigher hydrocarbons include benzene and hexene

^bLower hydrocarbons include CH₄, C₂H₄ and C₂H₆. Small amounts of C₃ oxygenates (include acetone, propanol, isopropanol) were produced in small amounts, too low to be accurately quantified

Fig. 6 Propene conversion under microwave heating (0.2 g of catalyst, propene:oxygen:nitrogen = 1:2:97, flow rate = 50 mL min⁻¹)

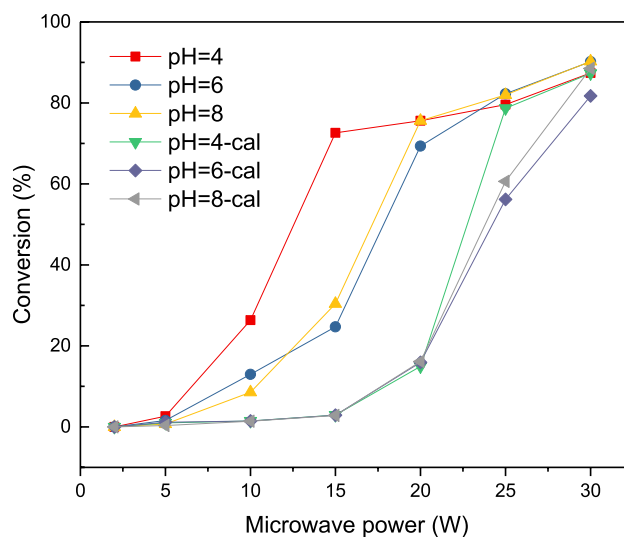
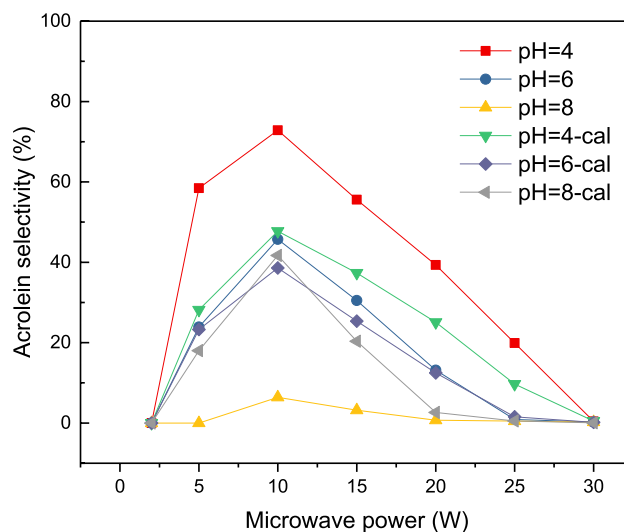


Fig. 7 Acrolein selectivity under microwave heating (0.2 g of catalyst, propene:oxygen:nitrogen = 1:2:97, flow rate = 50 mL min⁻¹)



be initially formed in high concentrations, but at longer reaction times can further converted to subsequent products, reducing the selectivity. To compare catalysts at isoconversion in continuous flow gas phase reactions the flow rate or catalyst amounts are adjusted to control the contact time.

In this study, a range of microwave powers and temperatures were used to explore the selectivity at different activities to allow a comparison of the two heating regimes under isoconversion. Experiments at isoconversion can be used to obtain kinetic data from reactions, although activation energies could not be calculated due to the difficulty in measuring the temperature accurately during the microwave assisted reactions. For the microwave-assisted process, the selectivity is similar at low conversions, but is much higher at conversions > 40%, giving twice the yield of acrolein at 70% conversion compared to conventional heating. This is attributed to the gas phase products not being heated once they desorb, reducing sequential reactions that lead to a loss in selectivity.

5 Conclusions

In this study, bismuth molybdate catalysts were found to be very active for the microwave-assisted selective oxidation compared to the same catalysts tested under conventional heating at isoconversion. The catalysts were synthesised using a hydrothermal method with citric acid, and the materials were tested before and after calcination for the selective oxidation of propene under both conventional and microwave-electric field heating.

Table 5 Selectivity of the main products from propene oxidation under microwave heating

| Sample | Input Power (W) | Selectivity (%) | | | | | |
|-----------|-----------------|--------------------|--------------|----------|---------------------------------|-----------------|---------------------|
| | | Lower hydrocarbons | Acetaldehyde | Acrolein | Other C ₃ oxygenates | CO _x | Higher hydrocarbons |
| BiMoOx-4 | 2 | 0 | 0 | 0 | 0 | 0 | 0 |
| | 5 | 0 | 6 | 59 | 34 | 0 | 0 |
| | 10 | 8 | 8 | 73 | 10 | 0 | 2 |
| | 15 | 8 | 6 | 55 | 8 | 21 | 1 |
| | 20 | 8 | 6 | 35 | 8 | 42 | 1 |
| | 25 | 13 | 6 | 19 | 2 | 55 | 4 |
| | 30 | 22 | 3 | 3 | 1 | 57 | 14 |
| BiMoOx-4C | 2 | 0 | 0 | 0 | 0 | 0 | 0 |
| | 5 | 0 | 6 | 28 | 66 | 0 | 0 |
| | 10 | 0 | 8 | 48 | 28 | 12 | 4 |
| | 15 | 0 | 8 | 37 | 17 | 34 | 4 |
| | 20 | 9 | 8 | 25 | 16 | 39 | 3 |
| | 25 | 23 | 5 | 10 | 4 | 41 | 17 |
| | 30 | 29 | 3 | 0 | 0 | 46 | 22 |
| BiMoOx-6 | 2 | 0 | 0 | 0 | 0 | 0 | 0 |
| | 5 | 0 | 7 | 24 | 68 | 0 | 0 |
| | 10 | 6 | 6 | 46 | 34 | 7 | 2 |
| | 15 | 13 | 6 | 30 | 21 | 19 | 12 |
| | 20 | 16 | 4 | 13 | 10 | 47 | 10 |
| | 25 | 18 | 3 | 1 | 12 | 47 | 18 |
| | 30 | 24 | 4 | 0 | 15 | 35 | 22 |
| BiMoOx-6C | 2 | 0 | 0 | 0 | 0 | 0 | 0 |
| | 5 | 0 | 6 | 23 | 71 | 0 | 0 |
| | 10 | 2 | 8 | 39 | 37 | 10 | 4 |
| | 15 | 11 | 9 | 25 | 31 | 19 | 5 |
| | 20 | 34 | 8 | 12 | 20 | 21 | 6 |
| | 25 | 31 | 5 | 2 | 11 | 32 | 19 |
| | 30 | 32 | 3 | 0 | 0 | 39 | 26 |
| BiMoOx-8 | 2 | 0 | 0 | 0 | 0 | 0 | 0 |
| | 5 | 16 | 23 | 0 | 27 | 0 | 34 |
| | 10 | 17 | 6 | 6 | 3 | 0 | 67 |
| | 15 | 19 | 0 | 3 | 1 | 24 | 53 |
| | 20 | 19 | 0 | 1 | 1 | 53 | 26 |
| | 25 | 20 | 0 | 0 | 0 | 48 | 31 |
| | 30 | 27 | 0 | 0 | 1 | 38 | 33 |
| BiMoOx-8C | 2 | 0 | 0 | 0 | 0 | 0 | 0 |
| | 5 | 0 | 23 | 18 | 27 | 0 | 32 |
| | 10 | 0 | 6 | 42 | 3 | 0 | 49 |
| | 15 | 11 | 0 | 20 | 1 | 24 | 42 |
| | 20 | 17 | 0 | 3 | 1 | 53 | 26 |
| | 25 | 28 | 0 | 1 | 0 | 48 | 22 |
| | 30 | 39 | 0 | 0 | 1 | 39 | 21 |

^aHigher hydrocarbons include benzene and hexene

^bLower hydrocarbons include CH₄, C₂H₄ and C₂H₆

^cC₃ oxygenates include acetone, propanol, isopropanol

Fig. 8 Acrolein yield under microwave heating (0.2 g of catalyst, propene:oxyg en:nitrogen = 1:2:97, flow rate = 50 mL min⁻¹)

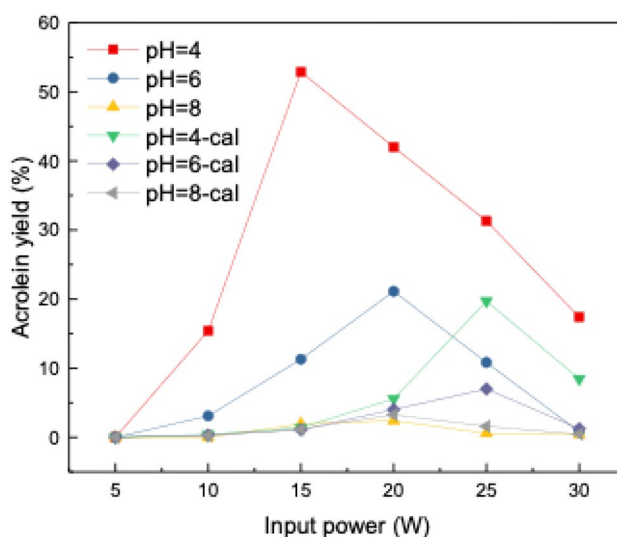


Fig. 9 Acrolein yield under conventional heating (0.2 g of catalyst, propene:oxyg en:nitrogen = 1:2:97, flow rate = 50 mL min⁻¹)

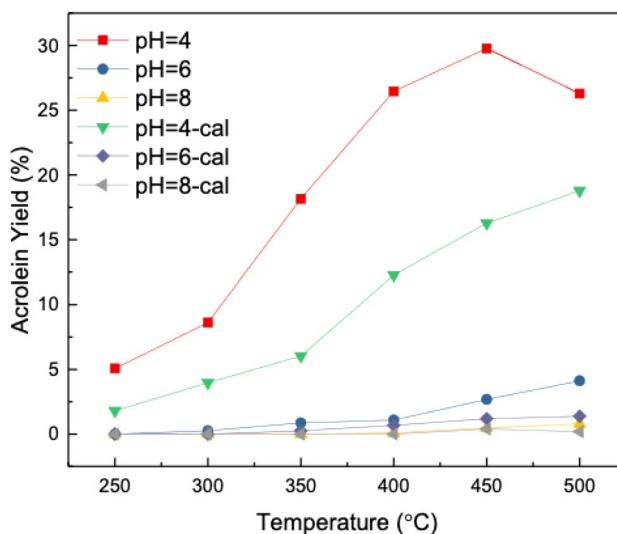
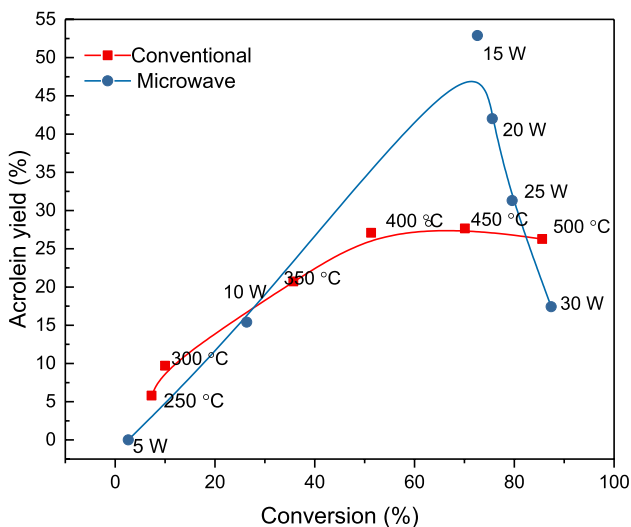


Fig. 10 Acrolein yield over BiMoOx-4 at different conversions under microwave heating and conventional heating (0.2 g of catalyst, propene:oxyg en:nitrogen = 1:2:97, flow rate = 50 mL min⁻¹)



Under conventional heating the synthesis pH of the hydrothermally prepared materials was found to be the most important factor, with catalysts prepared at pH 4 being the most active. Calcination at 500 °C did not change the composition of catalyst, but increased the crystallite size of the sample, resulting in a decrease in specific surface area and a reduced activity.

However, under microwave heating calcination was found to be the most important factor. Catalysts that were not calcined were found to have a high dielectric loss tangent, a measure of a materials ability to convert microwave-electric field radiation into heat, which was attributed to residual water and nitrate ions in the samples. Calcination led to a decrease in the dielectric loss tangent making the samples more difficult to heat. Under microwave heating the catalyst synthesised at pH 4 without calcination was the most active and selective and gave acrolein yields double that of the catalyst under conventional heating at 70% conversion.

This demonstrates the importance of the synthesis method when preparing catalysts for use in microwave-assisted catalysis, to be able to optimise both the active sites and dielectric properties of the materials. The best catalysts were found to be very selective to acrolein at high conversions which was attributed to the selective heating of the catalyst bed in the microwave field, minimising sequential oxidation reactions and cracking.

Acknowledgements UK Catalysis Hub is kindly thanked for resources and support provided via our membership of the UK Catalysis Hub Consortium and funded by EPSRC Grant EP/K014854/1.

Author contributions J.S. performed the experimental work assisted by J.S.H. and M.B., under the supervision of J.K.B. and D.R.S. J.K.B. and D.R.S. were responsible for funding acquisition. J.S. and J.K.B. wrote the main manuscript.

Funding The UK Catalysis Hub is kindly thanked for resources and support provided via our membership of the UK Catalysis Hub Consortium and funded by EPSRC Grant EP/K014854/1.

Data availability The datasets used and/or analysed during the current study are openly available through the Cardiff University Research Portal at <https://doi.org/10.17035/cardiff.29223230>.

Declarations

Ethics approval and consent to participate Not applicable.

Consent for publication Not applicable.

Competing interests The authors declare no competing interests.

Open Access This article is licensed under a Creative Commons Attribution 4.0 International License, which permits use, sharing, adaptation, distribution and reproduction in any medium or format, as long as you give appropriate credit to the original author(s) and the source, provide a link to the Creative Commons licence, and indicate if changes were made. The images or other third party material in this article are included in the article's Creative Commons licence, unless indicated otherwise in a credit line to the material. If material is not included in the article's Creative Commons licence and your intended use is not permitted by statutory regulation or exceeds the permitted use, you will need to obtain permission directly from the copyright holder. To view a copy of this licence, visit <http://creativecommons.org/licenses/by/4.0/>.

References

1. Gabriel C, Gabriel S, Grant EH, Halstead BSJ, Mingos DMP. Dielectric parameters relevant to microwave dielectric heating. *Chem Soc Rev*. 1998;27:213.
2. Stefanidis GD, Munoz AN, Sturm GSJ, Stankiewicz A. A helicopter view of microwave application to chemical processes: reactions, separations, and equipment concepts. *Rev Chem Eng*. 2014;30:233.
3. Palma V, Barba D, Cortese M, Martino M, Renda S, Meloni E. Microwaves and heterogeneous catalysis: a review on selected catalytic processes. *Catalysts*. 2020;10:246.
4. Slocombe DR, Porch A. *IEEE J Microw*. 2021;1:32.
5. Stankiewicz A, Sarabi FE, Baubaid A, Yan P, Nigar H. Perspectives of microwaves-enhanced heterogeneous catalytic gas-phase processes in flow systems. *Chem Rec*. 2019;19:40.
6. Le MT, Bismuth—Advanced Applications and Defects Characterization, InTech, 2018.
7. Swift HE, Bozik JE, Ondrey JA. Dehydrodimerization of propylene using bismuth oxide as the oxidant. *J Catal*. 1971;21:212–24.
8. Peacock JM, Parker AJ, Ashmore PG, Hockey JA. The oxidation of propene over bismuth oxide, molybdenum oxide, and bismuth molybdate catalysts: I. The preparation and testing of the catalysts. *J Catal*. 1969;15:373–8.
9. Batist P, Kinderen A, et al. The catalytic oxidation of 1-butene over bismuth molybdate catalysts: IV. Dependence of activity on the structures of the catalysts. *J Catal*. 1968;12:45–60.
10. Grasselli R, et al. Selective oxidation and ammoxidation of propylene by heterogeneous catalysis. *Adv Catal*. 1981;30:133–63.

11. Keulks G, Krenzke L, Catalysis TN-A. Selective oxidation of propylene. *Adv Catal.* 1979;28:183–225.
12. Krenzke L, Catalysis GK-J. The catalytic oxidation of propylene: VI. Mechanistic studies utilizing isotopic tracers. *J Catal.* 1980;61:316–25.
13. Carson D, Forissier M, Vedrine JC. Kinetic study of the partial oxidation of propene and 2-methylpropene on different phases of bismuth molybdate and on a bismuth iron molybdate phase. *J Chem Soc, Faraday Trans 1 Phys Chem Condens Phases.* 1984;80:1017–28.
14. Bettahar MM, Costentin G, Savary L, Lavalley JC. On the partial oxidation of propane and propylene on mixed metal oxide catalysts. *Appl Catal A.* 1996;145:1–48.
15. Sun J, Hayward JS, Barter M, Slocombe DR, Bartley JK. Designing heterogeneous catalysts for microwave assisted selective oxygenation. *ChemCatChem.* 2024;16: e202301586.
16. Wildberger MD, Grunwaldt JD, Maciejewski M, Mallat T, Baiker A. Sol–gel bismuth–molybdenum–titanium mixed oxides I. Preparation and structural properties. *Appl Catal A.* 1998;175:11–9.
17. Schuh K, Kleist W, Høj M, Trouillet V, Beato P, Jensen AD, Patzke GR, Grunwaldt J-D. Selective oxidation of propylene to acrolein by hydrothermally synthesized bismuth molybdates. *Appl Catal A.* 2014;482:145–56.
18. Cuenca JA, PhD Thesis, Cardiff University (UK), 2015.
19. Waldron RA. *Proc IEE C.* 1960;107:272.
20. Phuruangrat A, et al. Hydrothermal synthesis and characterization of Bi_2MoO_6 nanoplates and their photocatalytic activities. *J Nanomater.* 2013;2013:789705.
21. Bakiro M, Hussein Ahmed S, Alzamly A. Effect of pH, surfactant, and temperature on mixed-phase structure and band gap properties of BiNbO_4 nanoparticles prepared using different routes. *Chemistry.* 2019;1:89–110.
22. Mitchell AG, Lynek PM, Scott EF, Phillips CSG. Catalytic and surface-structural investigations of bismuth molybdate selective-oxidation catalysts. *J Chem Soc, Faraday Trans I.* 1981;77:2417–27.
23. Arora N, Deo G, Wachs IE, Hirt AM. Surface aspects of bismuth-metal oxide catalysts. *J Catal.* 1996;159:1–13.
24. Ravikumar Naik TR, Bhojya Naik HS. An efficient $\text{Bi}(\text{NO}_3)_3 \cdot 5\text{H}_2\text{O}$ catalyzed multi component one-pot synthesis of novel Naphthyridines. *Mol Divers.* 2008;12:139–42.
25. Bandyopadhyay D, Chavez A, Banik BK. Microwave-induced bismuth salts-mediated synthesis of molecules of medicinal interests. *Curr Med Chem.* 2017. <https://doi.org/10.2174/0929867324666170320121142>.
26. Bandyopadhyay D, Maldonado S, Banik BK. A microwave-assisted bismuth nitrate-catalyzed unique route toward 1,4-dihydropyridines. *Molecules.* 2012;17:2643–62.
27. Reilly LM, Sankar G, Catlow CRA. Following the formation of γ -phase Bi_2MoO_6 catalyst by in Situ XRD/XAS and thermogravimetric techniques. *J Solid State Chem.* 1999;148:178–85.
28. Christensen AN, Jensen TR, Scarlett NVY, Madsen IC, Hanson JC, Altomare A. In-situ X-ray powder diffraction studies of hydrothermal and thermal decomposition reactions of basic bismuth(iii) nitrates in the temperature range 20–650 °C. *Dalton Trans.* 2003. <https://doi.org/10.1039/B303926A>.
29. Zhang X, Hayward DO, Mingos DMP. Dielectric properties of MoS_2 and Pt Catalysts: effects of temperature and microwave frequency. *Catal Lett.* 2002;84:225–33.
30. Liu C, et al. Temperature and moisture dependence of the dielectric properties of silica sand. *J Microw Power Electromagn Energy.* 2013;47:199–209.
31. Keulks GW, Rosynek MP, Daniel C. Bismuth molybdate catalysts kinetics and mechanism of propylene oxidation. *Ind Eng Chem Prod Res Dev.* 1971;10:138–42.
32. Batist PA, Bouwens JFH, Schuit GCA. Bismuth molybdate catalysts. Preparation, characterization and activity of different compounds in the BiMoO system. *J Catal.* 1972;25:1–11.
33. Peacock JM, Parker AJ, Ashmore PG, Hockey JA. The oxidation of propene over bismuth oxide, molybdenum oxide, and bismuth molybdate catalysts. IV. The selective oxidation of propene. *J Catal.* 1969;15:398–406.
34. Martir W, Lunsford JH. The formation of gas-phase π -Allyl radicals from propylene over bismuth oxide and γ -bismuth molybdate catalysts. *J Am Chem Soc.* 1981;103:3728–32.
35. Schuh K, et al. Bismuth molybdate catalysts prepared by mild hydrothermal synthesis: Influence of pH on the selective oxidation of propylene. *Catalysts.* 2015;5:1554–73.
36. Schüth F, Ward MD, Buriak JM. Common pitfalls of catalysis manuscripts submitted to chemistry of materials. *Chem Mater.* 2018;30:3599–600.
37. Kapteijn F, Moulijn JA. Laboratory testing of solid catalysts. In: Ertl G, Knözinger H, Schüth F, Weitkamp J, editors. *Handbook of Heterogeneous Catalysis.* 2nd ed. Weinheim: Wiley; 2008. p. 2019–45.

Publisher's Note Springer Nature remains neutral with regard to jurisdictional claims in published maps and institutional affiliations.